Inorganic Chemistry
Article

Inorg. Chem. **2011**, *50*, 1521–1533 **1521**
DOI: 10.1021/ic101784w

Synthesis, Characterization, and Structural Studies of Multimetallic Ferrocenyl Carbene Complexes of Group VII Transition Metals

Daniela I. Bezuidenhout,* Simon Lotz, Marilé Landman, and David C. Liles

Department of Chemistry, University of Pretoria, Lynnwood Road, Pretoria 0002, South Africa

Received October 25, 2010

Fischer carbene complexes of the group VII transition metals (Mn and Re) containing at least two or three different transition metal substituents, all in electronic contact with the carbene carbon atom, were synthesized. The structural features and their relevance to bonding in the carbene multimetal compounds were investigated, as they represent indicators of possible reactivity sites in polymetallic carbene assemblies. For complexes of the type $[ML_x\{C(OR)R'\}]$ (ML_x = $MnCp(CO)_2$ or $Re_2(CO)_9$), ferrocenyl (Fc) was chosen as the R′ substituent, while the OR substituent was systematically varied between an ethoxy or a titanoxy group, to yield the complexes **1a** (ML_x = $MnCp(CO)_2$, R = Et, R′ = Fc), **2a** (ML_x = $MnCp(CO)_2$, R = $TiCp_2Cl$, R′ = Fc), **3a** (ML_x = $Re_2(CO)_9$, R = Et, R′ = Fc), and **4a** (ML_x = $Re_2(CO)_9$, R = $TiCp_2Cl$, R′ = Fc). Direct lithiation of the ferrocene with *n*-BuLi/TMEDA at elevated temperatures, followed by the Fischer method of carbene preparation, resulted in formation of the novel biscarbene complexes with bridging ferrocen-1,1′-diyl (Fc′) substituents $[\{\pi\text{-}Fe(C_5H_4)_2\text{-}C,C'\}\{C(OEt)ML_x\}_2]$ (**1b**, ML_x = $MnCp(CO)_2$; **3b**, ML_x = $Re_2(CO)_9$) or the unusual bimetallacyclic bridged biscarbene complexes $[\{\pi\text{-}TiCp_2O_2{-}O,O'\}\{\pi\text{-}Fe(C_5H_4)_2\text{-}C,C'\}\{CML_x\}_2]$ (**2b**, ML_x = $MnCp(CO)_2$; **4b**, ML_x = $Re_2(CO)_9$). The target compounds that were isolated displayed a variety of different geometric isomers and conformations. The greater reactivity of the binary dirhenium acylates in solution, compared to that of the cyclopentadienyl manganese acylate, resulted in a complex reaction mixture. Although the stabilization of hydroxycarbene or hydrido-acyl intermediates of dirhenium carbonyls could not be achieved, their existence in solution was confirmed by the isolation of $[(\pi\text{-}H)_2{-}(Re(CO)_4\{C(O)Fc\})_2]$ (**8**), the unique dichloro-bridged biscarbene complex *fac*-$[(\pi\text{-}Cl)_2\text{-}(Re(CO)_3\{C(OEt)Fc\})_2]$ (**6**), the known hydrido complex $[Re_3(CO)_{14}H]$ (**5**), the acyl complex $[Re(CO)_5\{C(O)Fc\}]$ (**7**), and the aldehyde-functionalized *eq*-$[Re_2(CO)_9\{C(OTiCp_2Cl)(Fc'CHO)\}]$ (**9**).

Introduction

The activation of simple organic molecules by more than one transition metal constitutes an area of research that has grown in importance.[1] The applications of carbenes as active or auxiliary ligands in organic synthesis and catalysis, however, are mostly focused on monocarbene systems,[2] and as far as we are aware, very few studies on multimetal carbene complexes have been recorded.[3] The first examples of carbene complexes containing three different transition metal substituents (Figure 1), all in electronic contact with the carbene carbon atom, were recently synthesized in our laboratories.[4] These multimetallic carbene complexes containing chromium with carbonyl ligands is representative of a class of Fischer carbene complexes that exhibit high stability. Unlike the metal clusters defined by Cotton et al.,[5] these complexes do not contain metal−metal bonds but, rather, metal fragments clustered around the carbene functionality.

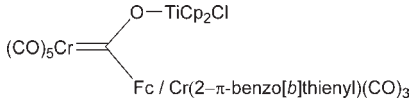

Figure 1. Chromium carbene multimetal complexes.

Whereas Fischer carbene synthesis is most successful with binary group VI metal carbonyl precursors, this reaction is complicated for carbonyl precursors of groups VII and IX, which require an X-type ligand for stability due to the uneven

*To whom correspondence should be addressed. Tel.: (+27) 12420 2626. Fax: (+27) 12420 4687. E-mail: daniela.bezuidenhout@up.ac.za.

(1) Thematic Issue: 2009 Carbenes Editorial, *Chem. Rev.* **2009**, *109*, 3209−3884 and references therein.

(2) (a) Garrison, J. C.; Simons, R. S.; Tessier, C. A.; Youngs, W. J. *J. Organomet. Chem.* **2003**, *673*, 1–4. (b) Fernández, I.; Mancheño, M. J.; Gómez-Gallego, M.; Sierra, M. A. *Org. Lett.* **2003**, *5*, 1237–1240. (c) Dötz, K. H.; Stendel, J. *Chem. Rev.* **2009**, *109*, 3227–3274. (d) Barluenga, J.; Santamaria, J.; Tomas, M. *Chem. Rev.* **2004**, *104*, 2259–2283.

(3) (a) Sierra, M. A. *Chem. Rev.* **2000**, *100*, 3591–3638. (b) Barluenga, J.; Fañanás, F. J. *Tetrahedron* **2000**, *56*, 4597–4628. (c) Fischer, E. O.; Fontana, S. *J. Organomet. Chem.* **1972**, *40*, 159–162. (d) Fischer, E. O.; Raubenheimer, H. G. *J. Organomet. Chem.* **1975**, *91*, C23–C26. (e) Balzer, B. L.; Cazanoue, M.; Sabat, M.; Finn, M. G. *Organometallics* **1992**, *11*, 1759–1763.

(4) Bezuidenhout, D. I.; van der Watt, E.; Liles, D. C.; Landman, M.; Lotz, S. *Organometallics* **2008**, *27*, 2447–2456.

(5) Cotton, F. A.; Wilkinson, G.; Murillo, C. A.; Bochmann, M. *Advanced Inorganic Chemistry*, 6th ed.; Wiley-Interscience: New York, 1999.

Published on Web 01/20/2011

Scheme 1. Synthesis of Manganese Carbene Complexes

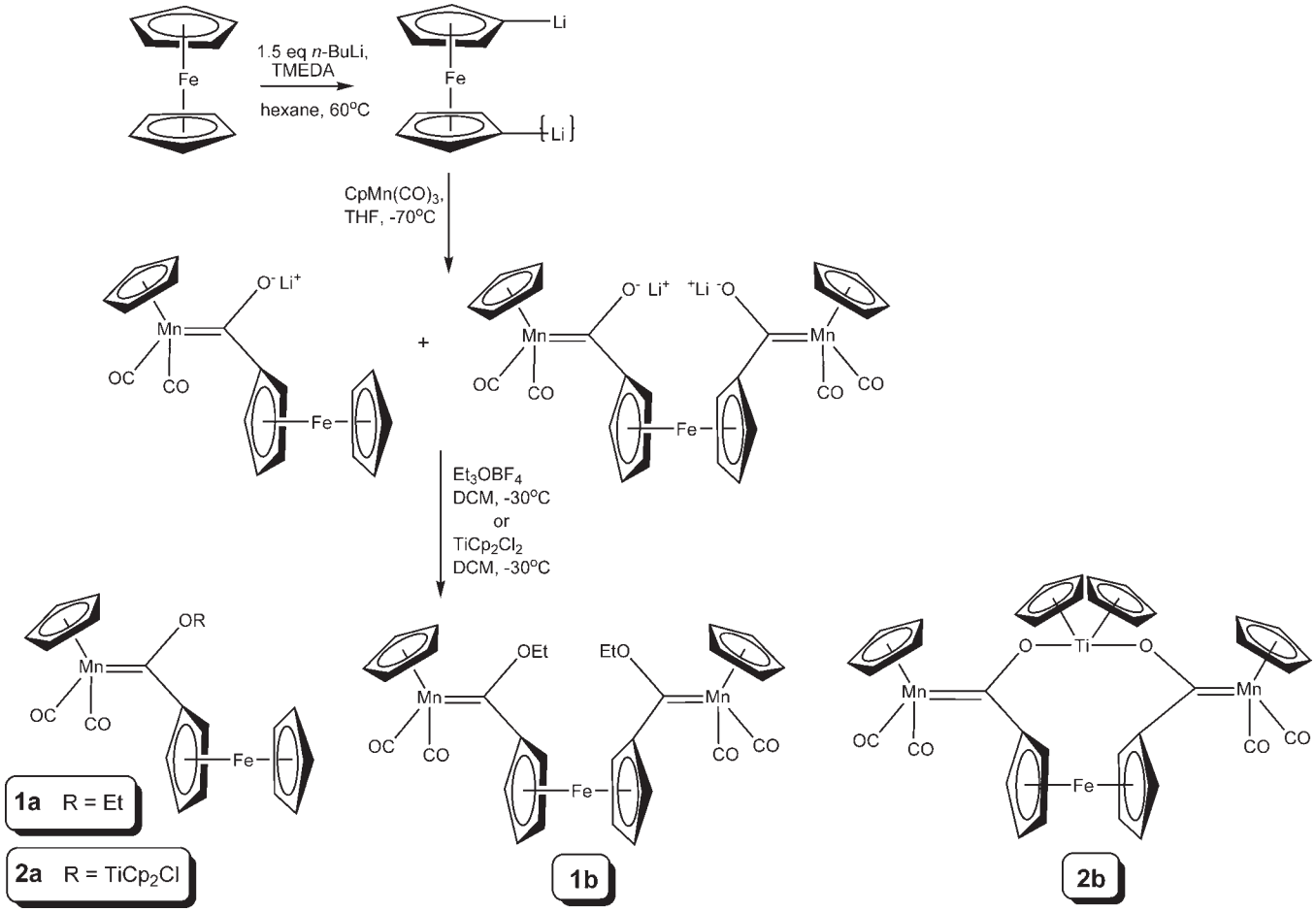

number of valence electrons.[3a,6] More reactive intermediates are therefore possible when group VII metal complexes react with nucleophiles due to the presence of both L- and X-type (Re−Re bonds, halogens, H, carbon groups excluding Cp) ligands in the precursors, compared to group VI metal carbonyl complexes. To expand this study beyond group VI transition metals, binary dirhenium decacarbonyl and the mononuclear [$MnCp(CO)_3$] precursor complexes were employed for the synthesis of multimetallic group VII carbene complexes, in an effort to investigate the character and reactivity of these metals (Mn, Re) toward the metal-substituted carbene ligands. The ferrocenyl group was chosen as a potential substituent, as it is known as an internal electron carrier.[7] The Lewis acid properties of titanocene dichloride prompted the use of this moiety as a third metal-containing fragment.[3b] The site of alkylation or protonation of transition metal acylates determines the reaction pathway, which affects the composition of products and can be divided into two types. *O*-alkylation/protonation (as seen for group VI transition metals) will lead to the formation of electrophilic Fischer carbene complexes.[3a,8] Metal alkylation/protonation (as seen for group VIII transition metals) will generally favor the formation of organic products since the subsequent elimination of ligands from the alkyl- or hydrido-acyl transition metal complexes affords the corresponding ketones or aldehydes.[6,9] For group VII transition metals, both pathways can occur, leading to a more complex range of products.

Results and Discussion

Synthesis and Spectroscopic Characterization of 1−9. The lithiation of ferrocene, when carried out with *n*-BuLi in hexane in the presence of TMEDA at 50 °C, gave a mixture of mono- and dilithiated ferrocene (LiFc, Li_2Fc'), typically in a 30:70 ratio. The dilithiated species precipitate from the solution as an orange solid. The yield relative to the monolithiated species can be increased (to above 80%) by careful removal of the solution. To obtain a higher yield of the monolithiated species, either lithiation

(6) (a) Fischer, E. O.; Kiener, V. J. *Organomet. Chem.* **1970**, *23*, 215–223. (b) Fischer, E. O.; Beck, H. J.; Kreiter, C. G.; Lynch, J.; Müller, J.; Winkler, E. *Chem. Ber* **1972**, *105*, 162–172. (c) Collman, J. P. *Acc. Chem. Res.* **1975**, *8*, 342–347. (d) Petz, W. *Organometallics* **1983**, *2*, 1044–1046. (e) Jiabi, C.; Guixin, L.; Weihua, X.; Xianglin, J.; Meicheng, S.; Yougi, T. *J. Organomet. Chem.* **1985**, *286*, 55–67. (f) Semmelhack, M. F.; Tamura, R. *J. Am. Chem. Soc.* **1983**, *105*, 4099–4100. (g) Lotz, S.; van Rooyen, P. H.; van Dyk, M. M. *Organometallics* **1987**, *6*, 499–505. (h) Conder, H. L.; York Darensbourg, M. *J. Organomet. Chem.* **1974**, *67*, 93–97.

(7) Connor, J. A.; Jones, E. M.; Lloyd, J. P. *J. Organomet. Chem.* **1970**, *24*, C20–C22.

(8) (a) Fischer, E. O. *Angew. Chem.* **1974**, *86*, 651–663. (b) Strassner, T. *Top. Organomet. Chem.* **2004**, *13*, 1–20.

(9) (a) Fischer, E. O.; Offhaus, E. *Chem. Ber.* **1967**, *100*, 2445–2456. (b) Fischer, E. O.; Offhaus, E.; Müller, J.; Nothe, D. *Chem. Ber.* **1972**, *105*, 3027–3035. (c) Alper, H.; Fabre, J.-L. *Organometallics* **1982**, *1*, 1037–1040. (d) Goldberg, K. I.; Bergman, R. C. *J. Am. Chem. Soc.* **1989**, *111*, 1285–1299. (e) Bergamo, M.; Beringhelli, T.; D'Alfonso, G.; Maggioni, D.; Mercandelli, P.; Sironi, A. *Inorg. Chim. Acta* **2003**, *350*, 475–485.

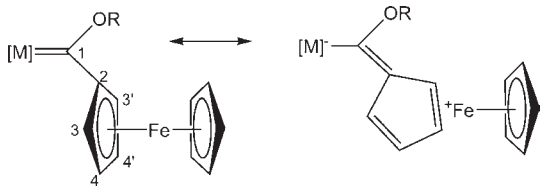

Figure 2. Resonance interaction between the ferrocene Cp ring and the carbene carbon atom.

in ether with *t*-BuLi affords the monolithiated product in over 80% yield[10] or the precursor bromomercuriferrocene[11] can be converted to iodoferrocene,[12] which yields the monolithiated ferrocene after metal−halogen exchange.[13] The general procedure followed in this study involved the reaction of *n*-BuLi with ferrocene to yield both the mono- and dilithiated precursors followed by the addition of the metal carbonyl substrate in THF at low temperatures, in line with previous studies with dilithiated thiophenes and the resulting synthesis of biscarbene rods.[14] The monocarbene complex of methylcyclopentadienyl manganese with ferrocenyl and ethoxy substituents on the carbene ligand has been synthesized before,[15] and the analogous cyclopentadienyl complex $[MnCp(CO)_2\{C(OEt)Fc\}]$ (**1a**) was synthesized in this study for the purpose of comparison. Alkylation with Et_3OBF_4 in dichloromethane yielded complex **1a** and the novel biscarbene complex **1b** $[\{\pi\text{-}Fe(C_5H_4)_2\text{-}C,C'\}\{C(OEt)MnCp(CO)_2\}_2]$. Alternatively, metalation with titanocene dichloride yielded the trimetallic monocarbene complex **2a** $[MnCp(CO)_2\{C(OTiCp_2Cl)Fc\}]$ and the double-bridged bisoxy titanocene ferrocen-1,1′-diyl complex **2b** $[\{\pi\text{-}TiCp_2O_2\text{−}O,O'\}\{\pi\text{-}Fe(C_5H_4)_2\text{-}C,C'\}\{CMnCp(CO)_2\}_2]$. The preparation of the manganese complexes is summarized in Scheme 1. Since the H3/H3′ protons, bonded to the cyclopentadienyl carbon atoms C3/C3′ (Figure 2), are closest to the site of coordination of the carbene carbon atom (labeled C1), the chemical shift of these protons is influenced most and is a sensitive probe for electronic ring substituent involvement with the carbene carbon atom. Significant downfield shifts of H3/H3′ were observed for the complexes compared to free ferrocene, indicating the electron-withdrawing effect of the metal carbonyl fragment bonded to the carbene ligand, as well as the π-delocalization of the ferrocene ring toward stabilizing the electrophilic carbene carbon atom, as illustrated in Figure 2. When the ethoxy substituent of the cyclopentadienyl manganese ethoxycarbene complexes is replaced by a titanoxy substituent (**2a**,**b**), the chemical shift of the H3/3′ protons is shifted upfield by 0.61−0.54 ppm compared to **1**(**a**,**b**), indicating the greater extent of oxygen stabilization toward the carbene carbon atom for the titanoxy substituent compared to the ethoxy group. This is rationalized by the predominant acyl character of the C−O bond (Figure 3) and the ionic nature of the Ti−O bond.

Figure 3. Acyl character of titanoxycarbene complexes.

For the synthesis of the dirhenium ethoxycarbene complex **3a**, Fish and Rosenblum's method[12] was followed to prepare FcI, and the exchange reaction of a stoichiometric amount of *n*-BuLi in ether at −70 °C resulted in a high yield of FcLi with no concurrent dilithiation. Subsequent reaction with $[Re_2(CO)_{10}]$ in THF at −50 °C, followed by alkylation with Et_3OBF_4 in dichloromethane yielded the dark red complex $[Re_2(CO)_9\{C(OEt)Fc\}]$ (**3a**) in high yield (Scheme 2). Unreacted $[Re_2(CO)_{10}]$ and ferrocene were separated from the reaction mixture by column chromatography. NMR spectroscopy revealed duplication of all of the ^1H and ^{13}C chemical shifts for complex **3**, and two-dimensional NMR experiments were used to distinguish between the two sets of signals. It was concluded from this information, as well as the presence of more than one set of overlapping carbonyl bands in the IR spectrum, that a mixture of the equatorial and the axial isomers was present in solution, as the steric bulk of the ferrocenyl substituent could hinder the electronically favored equatorial substitution. It is anticipated that the carbene in the axial position will have the Re atom more involved in π-backbonding because of poorer π interaction with the second Re−metal (Re−Re bond). As a result, less electron donation is expected from the Fc ligand, and upfield resonances for H3 and H4, compared to the equatorial isomer, are expected. The remote ethoxy CH_3 group is hardly influenced, and only one triplet is observed. However, integration of the signal confirmed the resonance as that of six hydrogens, therefore two CH_3 groups. Unfortunately, the two different isomers could not be separated, possibly due to the fact that the isomers are in equilibrium in solution.

For the preparation of **3b**, the corresponding biscarbene complex to **3a**, ferrocene was readily dilithiated with *n*-BuLi and TMEDA in hexane at 45 °C. The dilithiated species precipitate out of the solution as an orange solid, and the yield relative to the monolithiated species could be increased by removal of the solution *via* canula. After solvent evaporation and cooling to −50 °C, 2 mol equivalents of dirhenium decacarbonyl was added in THF, and alkylation with a stoichiometric amount of alkylating agent yielded, besides unreacted rhenium carbonyl, two fractions identified by thin layer chromatography. The dark brown target complex *eq*,*eq*-$[\{\pi\text{-}Fe(C_5H_4)_2\text{-}C,C'\}\{C(OEt)Re_2(CO)_9\}_2]$ (**3b**) was eluted as the second fraction from a silica gel column in a yield of 38% (Scheme 2). Unlike the monocarbene analogue, no evidence of an axial isomer was observed. For the two ferrocenyl ethoxycarbene rhenium complexes (mono-**3a** and bis-**3b**), the chemical resonances of the H3/3′ protons are very similar, with δ = 4.91 and 4.88, respectively.

(10) (a) Benkeser, R. A.; Goggin, D.; Schroll, G. A. *J. Am. Chem. Soc.* **1954**, *76*, 4025–4026. (b) Mayo, D. W.; Shaw, R. D.; Rausch, M. *Chem. Ind. London* **1957**, 1388–1389.

(11) (a) Helling, J. F.; Seyferth, D. *Chem. Ind. London* **1961**, 1568. (b) Seyferth, D.; Hoffman, H. P.; Burton, R.; Helling, J. F. *Inorg. Chem.* **1962**, *1*, 227–231.

(12) Fish, R. W.; Rosenblum, M. *J. Org. Chem.* **1965**, *30*, 1253–1254.

(13) Hedberg, F. L.; Rosenberg, H. *Tetrahedron Lett.* **1969**, *46*, 4011–4012.

(14) (a) Lotz, S.; Crause, C.; Olivier, A. J.; Liles, D. C.; Görls, H.; Landman, M.; Bezuidenhout, D. I. *Dalton Trans.* **2009**, 697–710. (b) Landman, M.; Görls, H.; Lotz, S. *Z. Anorg. Allg. Chem.* **2002**, *628*, 2037–2043.

(15) Connor, J. A.; Lloyd, J. P. *J. Chem. Soc., Dalton Trans.* **1972**, 1470–1476.

Scheme 2. Synthesis of Rhenium Carbene Complexes

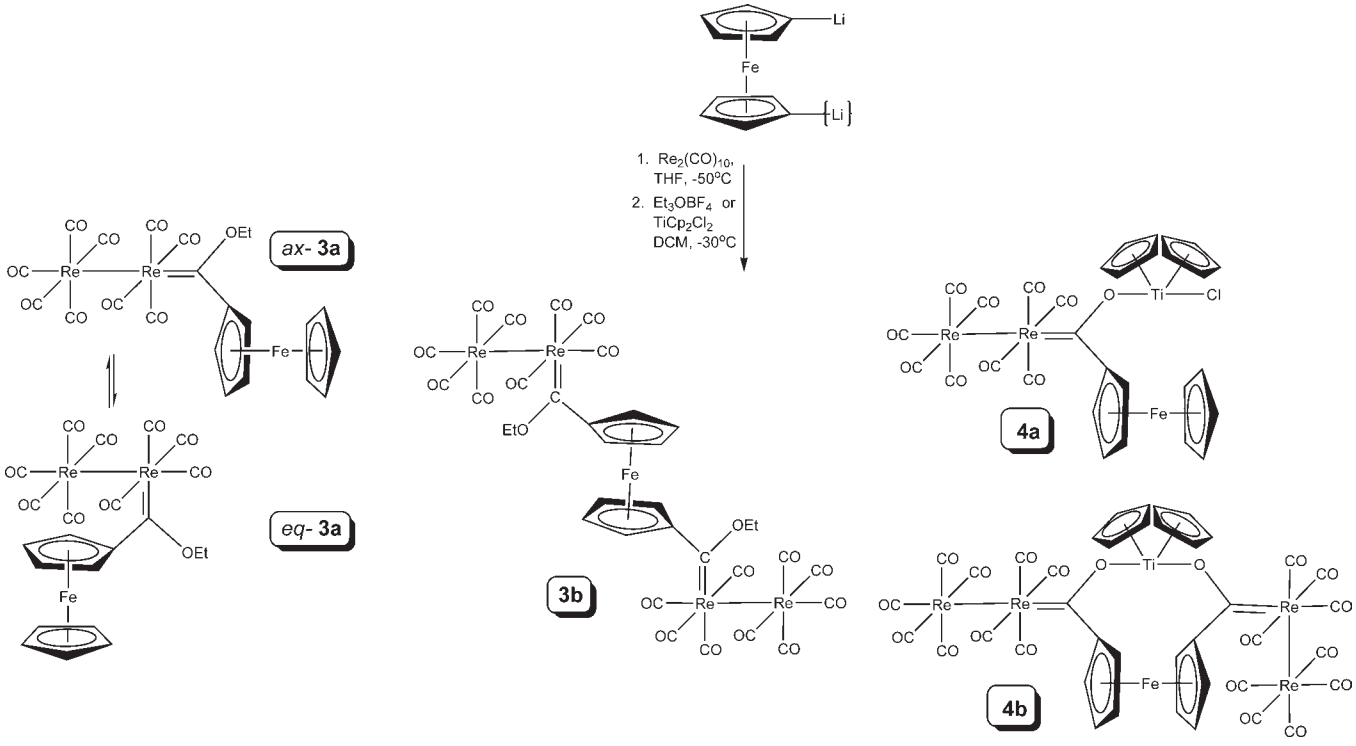

The same procedure as described above was employed to synthesize the titanoxycarbene complexes, the only difference being metalation of the acyl metalate with titanocene dichloride in dichloromethane, instead of alkylation with an oxonium salt, as illustrated in Scheme 2. Thin layer chromatography, after complexation with $TiCp_2Cl$, revealed the presence of nine different compounds, and these were separated and purified on an alumina column. The red monocarbene target complex **4a**, *ax*-[$Re_2(CO)_9$-{C(OTiCp_2Cl)Fc}], was eluted as the final fraction on the alumina column and proved to be the least stable of the Fischer carbene multimetal complexes. The assignment of an axial carbene ligand was based on the summarization of the carbonyl stretching modes by Ziegler et al.[16] The *eq*-[$M_2(CO)_9L$] displays a nine band pattern in the IR spectrum, corresponding to C_s symmetry. On the other hand, the IR spectrum of *ax*-[$M_2(CO)_9L$] with C_{4v} symmetry is observed to have only five bands. As expected, the ethoxycarbene complexes displayed carbonyl stretching vibrations at higher frequencies (see the Experimental Section), implying stronger M−C(carbene) backbonding compared to the titanoxycarbene complexes. Steric constraints imparted by the bulky $TiCp_2Cl$ substituent are assumed to be responsible for this unique substitution pattern, as the electronically favorable substitution site remains the equatorial site.[17]

The other target biscarbene complex, the hexametallic **4b** *ax*,*eq*-[{π-$TiCp_2O_2$-O,O′}{π-$Fe(C_5H_4)_2$-C,C′}{$CRe_2(CO)_9$}$_2$], was eluted as a dark brown-red fraction, having bridging ferrocen-1,1′-diyl and titandioxy substituents between the two carbene ligands. X-ray diffraction studies elucidated the interesting variation in the substitution site of the bridging biscarbene ligand: at one $Re_2(CO)_9$ fragment, the substitution is axial, whereas at the other, the substitution is equatorial. The remaining chloro ligand of the titanoxy substituent displays enhanced activation[18] and reacts with a second acylate oxygen to form **4b**. When comparing the ^{13}C NMR carbene carbon resonances of the ethoxycarbene complexes (**3a**,**b**) with those of the titanoxycarbene carbons (**4a**,**b**), a clear upfield shift of the titanoxy analogues would seem to support the conclusion that the titanoxy fragment better stabilizes the carbene carbon atom than an ethoxy group (similarly to the results obtained from proton NMR spectra and the comparison of the H3/3′ chemical shifts).

The formation of secondary products isolated from the reaction mixture can mostly be ascribed to the transfer of a proton by either an ionic or a radical mechanism. Before reaction with an electrophile, the lithiated salt can be represented either as a rhenium acylate (**A**, **B**; Scheme 3) that can be converted to the rhenium carbonyl anion by Re−Re bond cleavage, or as an acyl rhenium complex (**C**). The presence of [$Re(CO)_5H$] was indicated by a ^{1}H NMR signal at −5.8 ppm,[19] and *in situ* formation of the trirhenium hydride [$Re_3(CO)_{14}H$] (**5**), the so-called Fellman−Kaesz complex,[20] occurs, as shown in Scheme 4. The proton NMR spectrum showed an extreme upfield hydride shift at δ −15.41. The complex can be considered as $Re(CO)_5$ and $Re_2(CO)_9$ fragments bridged by a hydrido ligand. Byers and Brown[21] have suggested a radical

(16) Ziegler, M. L.; Haas, H.; Sheline, R. K. *Chem. Ber.* **1965**, *98*, 2454–2459.

(17) Bezuidenhout, D. I.; Liles, D. C.; van Rooyen, P. H.; Lotz, S. *J. Organomet. Chem.* **2007**, *692*, 774–783.

(18) Petz, W. *J. Organomet. Chem.* **1974**, *72*, 369–375.

(19) (a) Martin, B. D.; Warner, K. E.; Norton, J. R. *J. Am. Chem. Soc.* **1986**, *108*, 33–39. (b) Krumper, J. R.; Martin, R. L.; Hay, P. J.; Yung, C. M.; Veltheer, J.; Bergman, R. G. *J. Am. Chem. Soc.* **2004**, *126*, 14804–14815. (c) Adams, R. D.; Kwon, O.-S.; Perrin, J. L. *J. Organomet. Chem.* **2000**, *596*, 102–108.

(20) Fellman, W.; Kaesz, H. D. *Inorg. Nucl. Chem. Lett.* **1966**, *2*, 63–67.

mechanism for the formation of this complex, either from $Re_2(CO)_9H$ and $Re(CO)_5$ radicals or from $Re_2(CO)_9$ and $Re(CO)_5H$. In addition, a light yellow fraction obtained during the column chromatographic separation of the rhenium titanoxycarbene reaction mixture was identified as $[Re(CO)_5Cl]$. Evidence of chlorine abstraction from dichloromethane in a radical mechanism by a tetrahedrane cluster $[RCCo_2Mo(\eta^5\text{-indenyl})(CO)_8]$ (R = H; Ph), after breaking of the Mo−Co and Co−Co bonds, has recently been published by Watson et al.[22] Also, reaction of a ruthenium carbonyl complex $[Ru_2(CO)_2(\pi\text{-CO})\text{-}H(\pi\text{-CCPh})(\pi\text{-dppm})_2]$ with a chlorinated solvent, CH_2Cl_2, resulted in ligand substitution by a solvent chlorine atom to give $[Ru_2(CO)_2(\pi\text{-CO})Cl(\pi\text{-CCPh})(\pi\text{-dppm})_2]$.[23] Alternatively, labile chloride ions lost from the titanocene dichloride metalating agent could offer another source of the chlorine atom.

The second product isolated from the reaction of the rhenium carbonyl acylate with Et_3OBF_4 was shown by a single crystal X-ray structure determination to be *fac*-$[(\pi\text{-}Cl)_2\text{-}(Re(CO)_3\{C(OEt)Fc\})_2]$ (**6**). The formation of **6** can be rationalized by the transfer of a solvent chlorine and the concurrent breaking of the Re−Re bond to give the monorhenium chloro intermediate. Loss of a carbonyl ligand occurs, and two of the resultant coordinatively unsaturated *fac*-$[Re(CO)_3\{C(OEt)Fc\}Cl]$ molecules combine by means of bridging chloro ligands, as indicated in Scheme 5. The bridged bischloro ferrocenyl biscarbene **6** contains an X-π-L type ligand for each metal center, resulting in greater electron density available on the metal centers for back-donation toward the carbene carbon atom. This cascade effect infers less involvement of the ferrocenyl rings toward carbene stabilization, and a resultant higher field chemical shift of the α protons. The driving force of the Re−Re bond breaking can be ascribed to the fact that the Re−Re bond energy is far less than that of a Re−C(O) or Re−C(OEt)R bond, which again is lower than that of a Re−halide or Re−H bond.[24] For a *fac*-$M(CO)_3L_3$ octahedral complex, two IR active bands are expected, namely, the A_1 band (at higher frequency) and the E band, roughly twice the intensity of the A_1 band as well as being broader, due to partial lifting of the degeneracy by asymmetric ligands.[16] This pattern was not obtained. Instead, the four bands displayed the pattern expected for a *cis*-$M(CO)_4L_2$ system, containing two A_1 bands, a B_1 and a B_2 band that are IR active. This was ascribed to the precursor *cis*-$[Re(CO)_4\text{-}\{C(OEt)Fc\}Cl]$ that is present during the formation of **6**, as shown in Scheme 5.

Complex **7**, shown in Scheme 6, was identified as the acyl compound $[Re(CO)_5\{C(O)Fc\}]$, where the C=O chemical shift presents at 234.8 ppm, obtained from the reaction shown in Scheme 6. It has been previously synthesized by Beck et al.[25] by the reaction of FcCOCl and $[Re(CO)_5]^-$ and was structurally characterized. The formation of **C** (Scheme 3) in the reaction mixture is seen

Scheme 3. Re−Acylate, Re−Hydrido, and Re−Acyl Intermediates

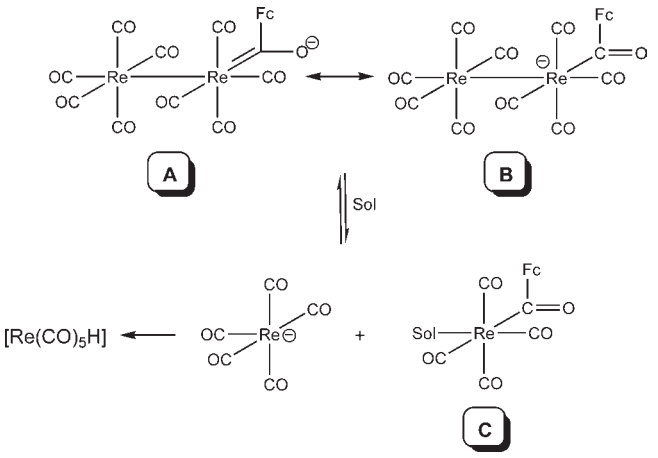

Scheme 4

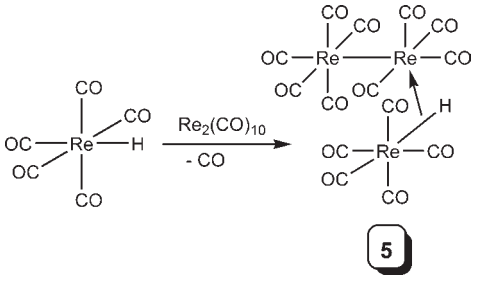

Scheme 5. Postulated Reaction Route for the Formation of **6** and Other Products

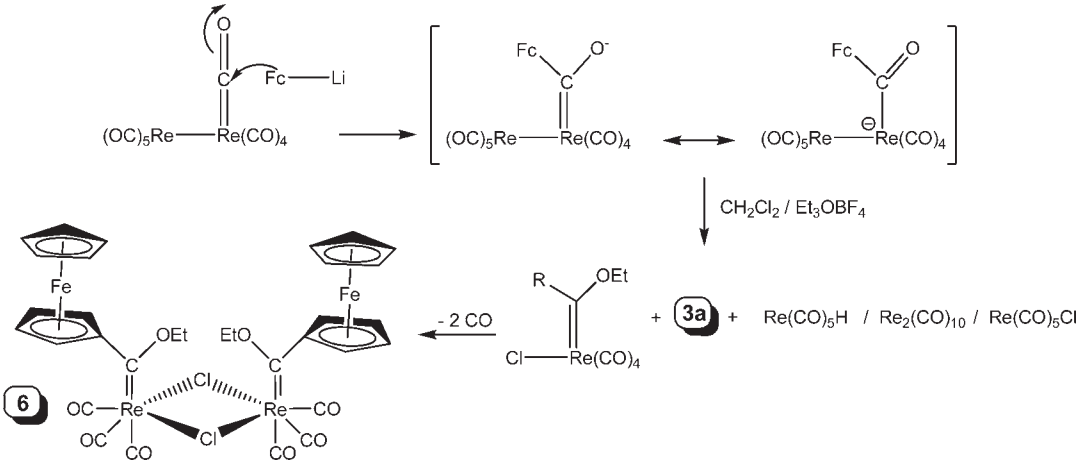

Scheme 6. Secondary Products Obtained from Reaction of Ferrocenyl Rhenium Acylate with $TiCp_2Cl_2$

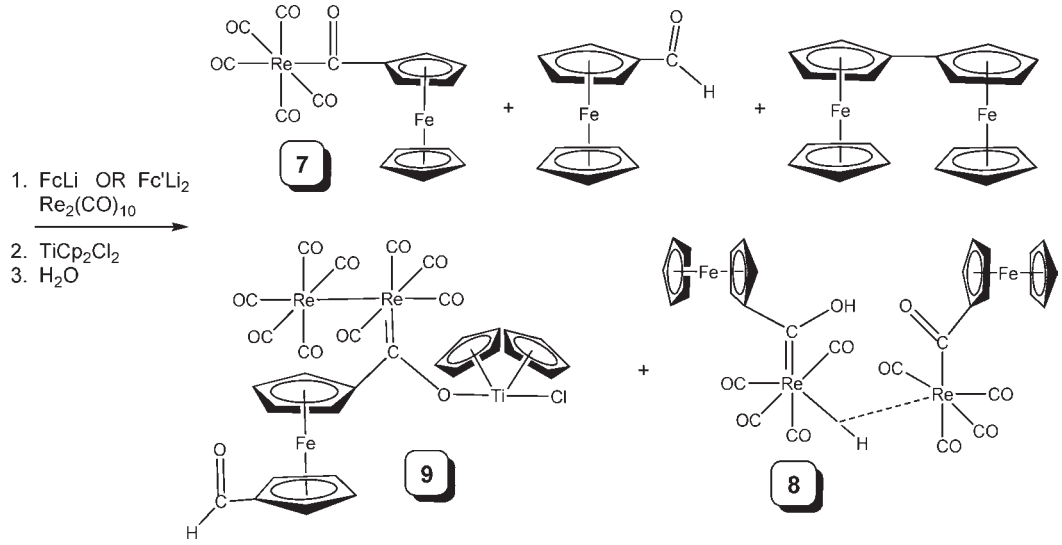

Scheme 7. Hydrogen Transfer Reactions Leading to **8**

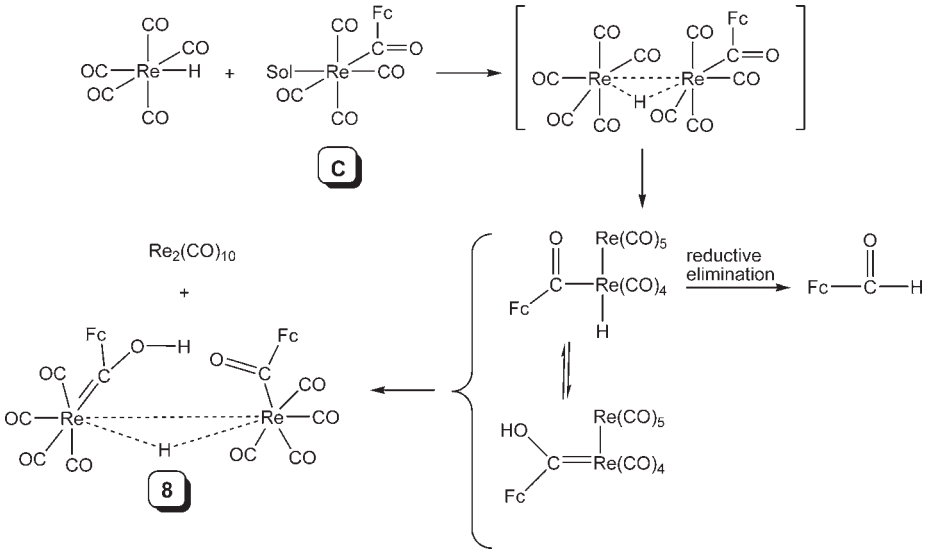

as a potential precursor to **7**, which is formed after the displacement of the coordinated solvent molecule by CO.

The transfer of a hydride to **C** by $[Re(CO)_5H]$ *via* a dirhenium intermediate with a bridging hydride or the protonation of the metal acylate **B** will give FcCHO after reductive elimination. A literature precedent for this is the kinetic study by Norton and co-workers for aldehyde formation from $[Re(CO)_5H]$ and $[Re(CO)_5CH_3]$.[26] This decomposition aldehyde (Scheme 7) was also isolated from the reaction mixture in this case and characterized by its NMR spectra as well as the characteristic C=O vibration in the IR spectrum at 1681 cm^{-1}.[27] A third route to acyl-hydride complexes is through hydroxycarbene complexes.[28] Hydrolysis of ethoxy or the more susceptible titanoxy substituents affords hydroxycarbene complexes and occurs during chromatography with polar solvents. Hydroxycarbene complexes can convert into aldehyde functionalities *via* the above equilibrium between the carbene and acyl-hydride intermediate. The

(21) Byers, B. H.; Brown, T. L. *J. Am. Chem. Soc.* **1977**, *99*, 2527–2532.
(22) Watson, W. H.; Poola, B.; Richmond, M. G. *J. Organomet. Chem.* **2006**, *691*, 5567–5575.
(23) Kuncheria, J.; Mirza, H. A.; Vittal, J. J.; Puddepatt, R. J. *J. Organomet. Chem.* **2000**, *593 − 594*, 77–85.
(24) (a) Connor, J. A. *Top. Curr. Chem.* **1977**, *71*, 71–110. (b) Collman, J. P.; Hegedus, L. S.; Norton, J. R.; Finke, R. G. *Principles and Application of Organotransition Metal Chemistry*; Oxford University Press: Mill Valley, CA, 1987.
(25) Breimair, J.; Wieser, M.; Wagner, B.; Polborn, K.; Beck, W. *J. Organomet. Chem.* **1991**, *421*, 55–64.
(26) (a) Martin, B. D.; Warner, K. E.; Norton, J. R. *J. Am. Chem. Soc.* **1986**, *108*, 33–39. (b) Warner, K. E.; Norton, J. R. *Organometallics* **1985**, *4*, 2150–2160. (c) Jones, W. D.; Bergman, R. G. *J. Am. Chem. Soc.* **1979**, *101*, 5447–5449.
(27) (a) Rosenblum, M. *Chem. Ind.* **1957**, *3*, 72. (b) Kamezawa, N. *J. Magn. Reson.* **1973**, *11*, 88–99.
(28) (a) Casey, C. P.; Czerwinski, C. J.; Hayashi, R. K. *J. Am. Chem. Soc.* **1995**, *117*, 4189–4190. (b) Casey, C. P.; Czerwinski, C. J.; Fusie, K. A.; Hayashi, R. K. *J. Am. Chem. Soc.* **1997**, *119*, 3971–3978. (c) Casey, C. P.; Czerwinski, C. J.; Powell, D. R.; Hayashi, R. K. *J. Am. Chem. Soc.* **1997**, *119*, 5750–5751. (d) Casey, C. P.; Nagashima, H. *J. Am. Chem. Soc.* **1989**, *111*, 2352–2353. (e) Casey, C. P.; Vosejpka, P. C.; Askham, F. R. *J. Am. Chem. Soc.* **1990**, *112*, 3713–3715.

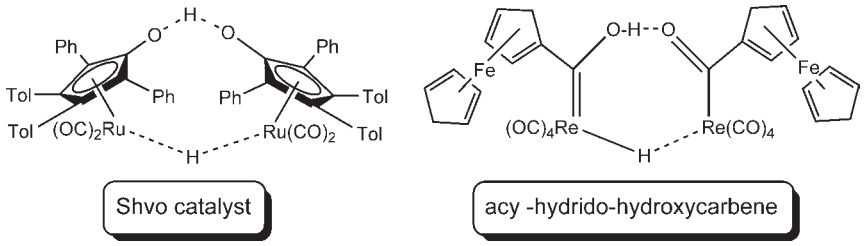

Figure 4. Complexes held together by protonic and hydridic hydrogens.

presence of the unique hydroxycarbene-acyl complex [(π-H)$_2$-(Re(CO)$_4${C(O)Fc}$)_2$] (**8**) was also identified by the molecular ion peak in the mass spectrum. As shown in Scheme 7, cleavage of the Re−Re bond of an intermediate species occurs to generate **8** and [$Re_2(CO)_{10}$]. Either Norton's H-transfer from [$Re(CO)_5H$][26] or the equilibrium between the hydroxycarbene and acyl-hydride intermediates observed by Casey[28] could result in the obtained product. Unlike in the Casey studies, however, no monorhenium hydroxycarbene or hydrido-acyl complexes could be isolated, and it was assumed that the equilibrium whereby the hydroxycarbene was converted into the acyl-hydride intermediate is favored. Complex **8** is unusual in that it exhibits a hydroxycarbene trapped in a dinuclear acyl-hydroxycarbene and also displays a bridging rhenium hydride. The carbene heteroatom substituent therefore cannot contribute toward π-stabilization of the carbene, and much greater influence is felt on the ferrocenyl ring. Notable is the resemblance of **8** to the well-known ruthenium Shvo catalyst (Figure 4).[29] Both complexes feature pendant oxygen atoms with a protonic hydrogen between them, as well as a bridging hydride holding together the two fragment complexes. The two most significant signals in the ^{1}H NMR spectrum are the highfield and lowfield signals that correspond to the hydridic and the protonic hydrogen atoms of the complex, where the bridging hydride value of −15.59 ppm is in good agreement with the value obtained for the Shvo catalyst (δ −17.9).[29] In the ^{13}C NMR spectrum, both the acyl (δ 231.5) and the extremely downfield hydroxycarbene signal (δ 346.2) are observed.

The isolation of the dimerization product biferrocene[30] (Scheme 6) and FcCHO can be rationalized by the ionic nature of the titanoxy substituent, which would favor the rhenium acylate form of the intermediate (Figure 3) because of enhanced backbonding from the anionic oxygen to the electrophilic carbene carbon. The ionic nature of titanoxycarbene complexes is supported by the ease of hydrolysis of this metal fragment and by the structural studies, so that the titanoxycarbene complex can be viewed as an acyl synthon comparable to the situation observed by Barluenga and co-workers for [$Mo(CO)_5${C(OBX$_2$)R}].[31]

A final product was isolated, albeit in a very low yield (< 5%), and was identified as *eq*-[$Re_2(CO)_9${C(OTiCp$_2$Cl)(Fc′CHO)}] (**9**), formed from a dilithiated ferrocene

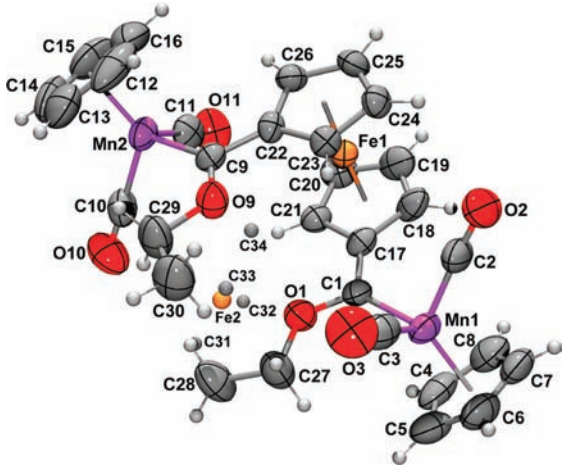

Figure 5. ORTEP + POV-Ray drawing of the molecular structure of **1b**. Atomic displacement ellipsoids are shown at the 50% probability level. The iron and carbon positions (Fe2, C31−C34) needed to complete the ferrocenyl group of a minor (8%) orientation of the molecule (with the ferrocenyl and the two ethoxy entities swapped) are shown as arbitrary sized spheres.

precursor, with reductive elimination of the $Re_2(CO)_9$ moiety only occurring on one side of the ferrocene, the other retaining its [$Re_2(CO)_9${C(OTiCp$_2$Cl)] metal carbene fragment (Scheme 6). Equatorial substitution of the carbene ligand was assigned from the IR spectrum of this compound. As has been observed from **4a** and **4b**, both equatorial (electronically favored) and axial substitution (sterically favored) are possible. The two modified rhenium carbene complexes, **8** and **9**, display greater downfield shifts of H3/3′ than in any other case (δ 4.92 and 5.03, respectively).

The formation of products in Schemes 4−7 can be accounted for by homolytic bond cleavage into fragment radicals, which can be combined again to give the products, as demonstrated by the observance of FcCHO and biferrocene as fragment ions in the mass spectra of compounds **8** and **9**. The presence of a high intensity peak for the [M−$Re(CO)_5$]$^+$ fragment in all compounds containing a $Re_2(CO)_9$ moiety also indicates the low bond strength of the Re−Re bond.

Crystal and Molecular Structures of Complexes 1b, 3b, 4b, and 6. Single crystals of suitable quality were obtained for the biscarbene complexes **1b**, **3b**, **4b**, and **6**. X-ray diffraction studies confirmed the molecular structures of these compounds. The complexes were crystallized by solvent layering of different ratios of hexane on a dicloromethane solution of the complex. Complex **3b** crystallized with two molecules in the asymmetric unit. There are no significant differences in the molecular structures of the two independent molecules. Complex **4b** crystallized as a

(29) (a) Shvo, Y.; Czarkie, D.; Rahamim, Y. *J. Am. Chem. Soc.* **1986**, *108*, 7400–7402. (b) Casey, C. P.; Powell, D. R.; Hayashi, R. K.; Kavana, M. *J. Am. Chem. Soc.* **2001**, *123*, 1090–1100. (c) Bullock, R. M. *Chem.—Eur. J.* **2004**, *10*, 2366–2374.

(30) (a) Rausch, M. D.; Vogel, M.; Rosenberg, H. *J. Org. Chem.* **1957**, *22*, 900–903. (b) Rausch, M. D. *J. Am. Chem. Soc.* **1960**, *82*, 2080–2081.

(31) Barluenga, J.; Rodríguez, F.; Fañanás, F. J. *Chem.—Eur. J.* **2000**, *6*, 1930–1937.

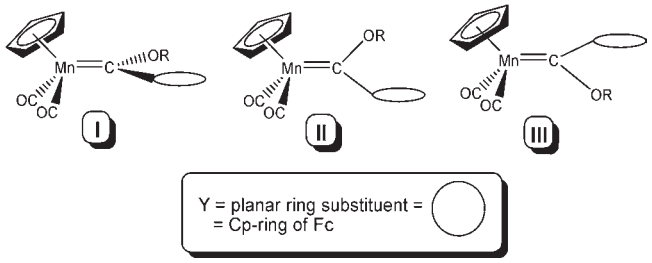

Figure 6. Possible conformations of carbene complexes $[MnCp(CO)_2\{C(OR)Y\}]$.

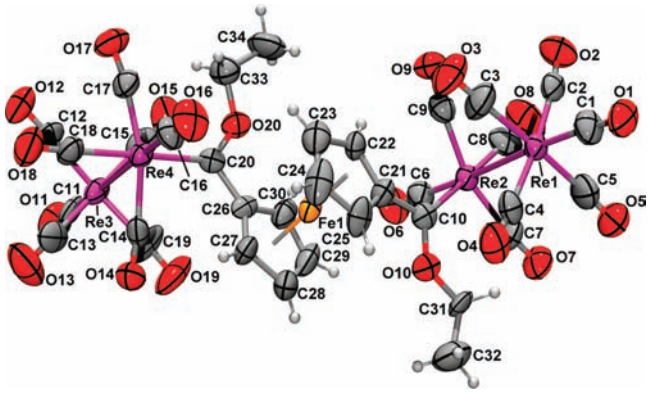

Figure 7. ORTEP + POV-Ray drawing of the molecular structure of one independent molecule of **3b**. The numbering scheme for the second molecule may be derived by adding 40 to each of the atom numbers shown. Atomic displacement ellipsoids are shown at the 50% probability level.

dihydrate. The hydrogen atoms of the water molecules were not located. Crystals of **6** were also solvated with one molecule of dichloromethane per two molecules of the complex. ORTEP[32] + POV-Ray[33] drawings of the molecular structures are presented in Figures 5 and 7−9, showing the atom numbering schemes employed. Only one of the two independent molecules is shown for complex **3b** (Figure 7). The numbering scheme for the second molecule may be derived by adding 40 to each of the atom numbers shown. Crystallographic data, refinement parameters, and experimental details are given in the Experimental Section. Selected bond lengths, bond angles, and torsion angles are given for the manganese biscarbene complex **1b** in Table 1 and for the rhenium biscarbene complexes (**3b**, **4b**, and **6**) in Tables 2 and 3.

In the crystal structure of **1b** (Figure 5), the space occupied by the two ethoxy groups, which lie one above the other, is similar to that occupied by the ferrocenyl group. Thus, one enantiomer of the complex can occupy the crystal space of the other enantiomer with three of the carbon atoms in each Cp ring nearly coinciding with the non-hydrogen atom positions of the two ethoxy groups. Thus, the crystal structure is disordered with 8(2)% of the alternative enantiomer occupying the site of each molecule. The minor position occupied by the iron atom and the four carbon atom positions needed to complete the two Cp rings are shown as small spheres in Figure 5. The

(32) Farrugia, L. J. *J. Appl. Crystallogr.* **1997**, *30*, 565–565.
(33) The POV-Ray Team, POV-Ray 2004. URL: http://www.povray.org/download/ (accessed Jan 2011).

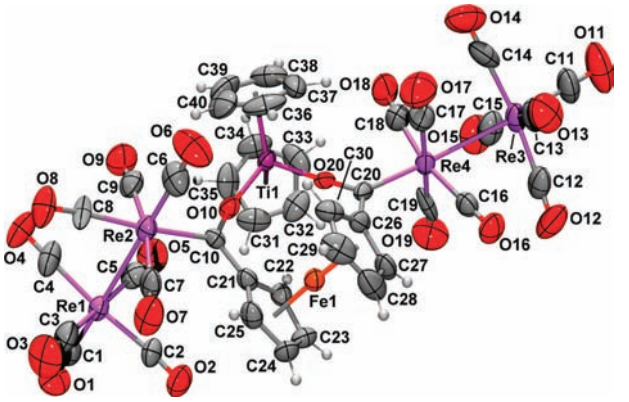

Figure 8. ORTEP + POV-Ray drawing of the molecular structure of **4b**. Atomic displacement ellipsoids are shown at the 50% probability level.

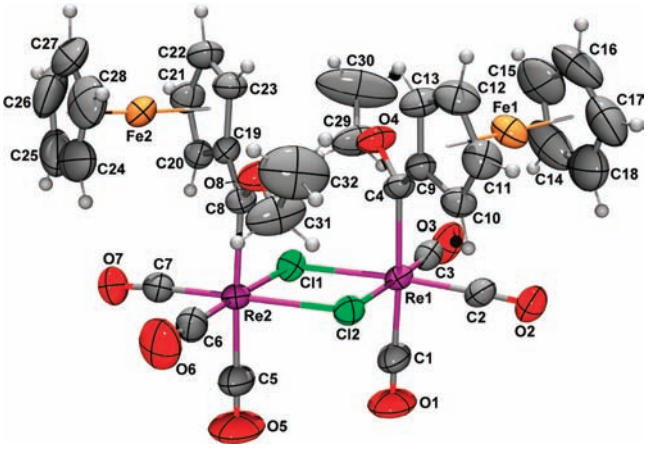

Figure 9. ORTEP + POV-Ray drawing of the molecular structure of **6**. Atomic displacement ellipsoids are shown at the 50% probability level.

molecule has approximate C_2 symmetry, and thus the corresponding bond lengths, bond angles, and torsion angles surrounding the two carbene carbon atoms are approximately equivalent. In $[MnCp(CO)_2\{C(OR)Y\}]$ complexes, with two different organic substituents R and Y (Y = planar ring substituent), there are three possible conformations (**I**, **II**, and **III** in Figure 6) as far as the mutual orientation of the carbene plane and the $MnCp(CO)_2$ moiety is concerned. In contrast to the calculated findings of Kostić and Fenske,[34] and comparison of known structures of $[MnCp(CO)_2(carbene)]$ complexes,[35] where conformation **II** (with the carbene plane approximately coplanar with the psudo-mirror plane of the $MnCp(CO)_2$ fragment) was found to be the most stable, the structure of **1b** has the carbene plane approximately perpendicular to the psudo-mirror plane of the $MnCp(CO)_2$ fragment (with approximately C_s symmetry) and thus has conformation **I**. Only two other structures exhibit

(34) Kostić, N. M.; Fenske, R. F. *Organometallics* **1982**, *1*, 974–982.
(35) (a) Schubert, U. *Organometallics* **1982**, *1*, 1085–1088. (b) Malisch, W.; Blau, H.; Schubert, U. *Angew. Chem.* **1980**, *92*, 1065–1066. (c) Malisch, W.; Blau, H.; Schubert, U. *Chem. Ber.* **1983**, *116*, 690–709. (d) Fischer, E. O.; Kleine, W.; Schambeck, W.; Schubert, U. *Z. Naturforsch., B.: Anorg. Chem. Org. Chem.* **1981**, *36B*, 1575. (e) Friedrich, P.; Besl, G.; Fischer, E. O.; Huttner, G. *J. Organomet. Chem.* **1977**, *139*, C68–C72. (f) Herrmann, W. A.; Weidenhammer, K.; Ziegler, M. L. *Z. Anorg. Allg. Chem.* **1980**, *460*, 200–206. (g) Fontana, S.; Schubert, U.; Fischer, E. O. *J. Organomet. Chem.* **1978**, *146*, 39–44.

conformation **I**: $[MnCp(CO)_2\{C(OMe)menthyl\}]$[35g] and $[Mn((MeCp)(CO)_2\{C(OMe)PMe_3\}]$.[35b] In all of these complexes, the carbene carbon carries bulky substituents, forcing the carbene plane to orient in a less favorable way with respect to the $MnCp(CO)_2$ fragment. Conformation **I** was not observed in the case of biscarbene complexes.[36]

$MnCp(CO)_2$ moieties exhibit high back-bonding ability and supply sufficient electron density to the carbene carbon so that π-donating organic substituents at the carbene carbon are not essential to stabilize these types of complexes. A structural consequence of the above statement is the longer C(carbene)−O bond distance (1.340(5) Å) than for group VI alkoxycarbene complexes in which alkoxy groups serve as π-donating substituents.[35a] The ethoxy group poorly competes with the $MnCp(CO)_2$ moiety for π-bonding with the carbene carbon. This is also true for most other $[MnCp(CO)_2(carbene)]$ complexes; however, a significantly longer Mn−C(carbene) bond length is found for **1b** than for other reported cyclopentadienyl manganese carbene complexes.[35] In most cases, the Mn−C(carbene) bond distance was reported as being in the range 1.85−1.87 Å and is not significantly influenced by the nature of the organic substituents. For the ferrocenyl-substituted **1b**, Mn−C(carbene) distances of 1.924(5) and 1.916(5) Å were observed, thereby a considerable π-donating ability of the ferrocenyl substituent can be inferred, as less back-donation from the $MnCp(CO)_2$ fragment is required.

Table 1. Selected Bond Lengths (Å), Bond Angles (deg), and Torsion Angles (deg) for **1b**

bond lengths		bond angles	
Mn1−C1	1.924(5)	Mn1−C1−O1	127.1(3)
Mn2−C9	1.916(5)	Mn2−C9−O9	128.7(3)
C1−O1	1.340(5)	Mn1−C9−C17	126.3(3)
C9−O9	1.338(5)	Mn2−C9−C22	126.4(3)
C1−C17	1.447(6)	O1−C1−C17	106.3(4)
C9−C22	1.447(6)	O9−C9−C22	104.4(4)
O1−C27	1.440(5)	C1−O1−C27	123.1(4)
O9-C29	1.450(6)	C9−O9−C29	122.1(4)
Mn1−C(2,3)[a]	1.759(6)	C1−C17−C18	127.1(4)
Mn2−C(10,11)[a]	1.763(6)	C9−C22−C23	128.2(4)
C(2,3)−O(2,3)[a]	1.170(6)	C1−C17−C21	127.7(4)
C(10,11)−O(10,11)[a]	1.157(7)	C9−C22−C26	127.0(4)
torsion angles			
C2−Mn1−C1−O1			−144.7(4)
C10−Mn2−C9−O9			−50.1(4)
Mn1−C1−C17−C18			−5.0(6)
Mn2−C9−C22−C26			−5.2(6)
O1−C1−C17−C21			4.7(6)
O9−C9−C22−C23			5.1(6)

[a] Averaged value.

For complexes of the type $[Re_2(CO)_9(carbene)]$, the favored electronic position for the carbene ligand is *cis* to the rhenium−rhenium bond. Neutral rhenium carbonyl complexes require one X-type ligand, which is a bulky $Re(CO)_5$ fragment in complexes **3b** and **4b**. Thus, the carbene ligand should lie in the equatorial plane and be in a staggered conformation with respect to the carbonyl ligands of the equatorial plane of the other $Re(CO)_5$ group. This is true for **3b** (Figure 7) but not for **4b** (Figure 8). The geometries of the two rhenium−carbene carbon termini in the biscarbene complexes **3b** and **6** (Figure 9) are approximately equivalent, but complex **4b** is exceptional in that one of the carbene ligands has sacrificed the electronic favored equatorial position for an axial position. This is one of the rare examples of dirhenium nonacarbonyl complexes deviating from equatorially coordinated ligands, as previously noted by Takaya et al. in their report of an axial titanoxy monocarbene complex of rhenium nonacarbonyl.[37] Fischer and Rustemeyer[38] reported a rhenium octacarbonyl complex containing two carbene ligands and found one of the carbene ligands in an equatorial and the other in an axial position, *eq*,*ax*-$[\{Re(CO)_4\{C(OEt)SiPh_3\}\}_2]$. In **6**, there are only two monorhenium fragments, but the orientations are nevertheless retained through the two bridging chloro ligands. The Re···Re nonbonding distance is *ca.* 0.8 Å longer than the Re−Re bonds because of these bridging chloro ligands.

The rhenium−carbene distances listed in Table 2 are consistent with a double bond character and with an

Table 2. Selected Bond Lengths (Å) of Ferrocenyl Rhenium Biscarbene Complexes **3b**, **4b**, and **6**

bond lengths	**3b**	**3b** atom # + 40	**4b**	bond lengths	**6**
Re1−Re2	3.0974(9)	3.0771(9)	3.0712(8)	Re1−Re2	3.9046(4)
Re3−Re4	3.0632(9)	3.0962(9)	3.0569(8)		
Re1−C1	1.924(19)	1.904(19)	1.912(17)	Re1−C1	1.953(7)
Re3−C11	1.93(2)	1.93(2)	1.912(18)	Re2−C5	1.959(8)
Re2−C10	2.111(15)	2.100(14)	2.178(11)	Re1−C4	2.171(6)
Re4−C20	2.108(14)	2.090(15)	2.059(13)	Re2−C8	2.166(6)
C10−O10	1.355(17)	1.319(17)	1.286(14)	C4−O4	1.321(7)
C20−O20	1.327(16)	1.324(17)	1.272(14)	C8−O8	1.324(7)
C10−C21	1.460(19)	1.44(2)	1.448(17)	C4−C9	1.437(9)
C20−C26	1.493(19)	1.502(19)	1.481(18)	C8−C19	1.441(8)
O10−C3	1.449(16)	1.471(18)		O4−C29	1.451(9)
O20−C33	1.444(18)	1.440(19)		O8−C31	1.457(9)
O10−Ti1			1.968(9)		
O20−Ti1			1.929(8)		
Re2−C(6,7,8,9)[a]	1.958(19)	1.966(16)	1.949(16)	Re1−C(2,3)[a]	1.888(7)
Re4−C(16,17,18,19)[a]	1.952(18)	1.973(18)	1.936(18)	Re2−C(6,7)[a]	1.890(8)
				Re1−Cl1	2.5252(15)
				Re1−Cl2	2.5289(15)
				Re2−Cl1	2.5249(15)
				Re2−Cl2	2.5351(15)

[a] Averaged value.

Table 3. Selected Bond Angles (deg) and Torsion Angles (deg) of Ferrocenyl Rhenium Biscarbene Complexes **3b**, **4b**, and **6**

bond angles	**3b**	**3b** atom # + 40	**4b**	bond angles	**6**
Re1−Re2−C10	84.2(4)	89.1(4)	95.0(3)		
Re3−Re4−C20	90.7(4)	81.4(4)	175.1(3)		
Re2−C10−O10	129.2(10)	131.3(10)	120.6(8)	Re1−C4−O4	127.07(4)
Re4−C20−O20	128.7(10)	130.4(10)	125.7(10)	Re2−C8−O8	127.29(4)
Re2−C10−C21	125.9(12)	124.4(11)	126.4(8)	Re1−C4−C9	125.35(5)
Re4−C20−C26	126.4(11)	123.3(11)	120.6(8)	Re2−C8−C19	125.02(5)
C10−O10−C31	122.0(12)	122.7(12)		C4−O4−C29	123.81(6)
C20−O20−C33	125.5(12)	123.6(12)		C8−O8−C31	124.38(6)
C10−O10−Ti1			161.3(8)		
C20−O20−Ti1			176.2(8)		
C10−Re2−C6	89.0(7)	90.0(7)	87.6(5)	C4−Re1−C3	93.7(3)
C20−Re4−C16	90.1(6)	90.0(7)	97.4(5)	C8−Re2−C7	93.9(2)
C10−Re2−C8	177.1(6)	174.3(6)	172.2(8)	C1−Re1−C4	175.9(3)
C20−Re4−C18	175.3(7)	176.0(7)		C5−Re2−C8	176.6(3)
O10−C10−C21	104.8(13)	104.2(12)	113.0(10)	O4−C4−C9	107.4(5)
O20−C20−C26	104.9(12)	106.3(13)	112.8(11)	O8−C8−C19	107.6(5)
				Re1−Cl1−Re2	101.28(5)
				Re1−Cl2−Re2	100.90(5)
torsion angles	**3b**	**3b** atom # + 40	**4b**	torsion angles	**6**
C6−Re2−C10−O10	91.6(14)	100.6(14)	103.8(9)	C3−Re1−C4−O4	50.7(6)
C16−Re4−C20−O20	−91.56(1)	−90.3(15)	−175.57(1)	C6−Re2−C8−O8	45.6(6)
Re2−C10−C21−C22	17(2)	−150.7(14)	156.8(10)	Re1−C4−C9−C10	14.35(1)
Re4−C20−C26−C27	−23(2)	−34(2)	−56.0(17)	Re2−C8−C19−C20	10.2(9)
Re2−C10−C21−C25	−164.0(12)	33(2)	−21.6(19)	Re1−C4−C9−C13	179.23(5)
Re4−C20−C26−C30	163.3(11)	150.5(16)	−48.6(17)	Re2−C8−C19−C23	−179.5(5)
Re2−C10−O10−C31	−1(2)	−14(2)		Re1−C4−O4−C29	−10.67(9)
Re4−C20−O20−C33	14(2)	1(2)		Re2−C8−O8−C31	−6.93(9)
Re2−C10−O10−Ti1			121.43(2)		
Re4−C20−O20−Ti1			−89.54(12)		

Table 4. Data Collection and Crystal Structure Details

	1b	**3b**	**4b**	**6**
formula	$C_{30}H_{28}FeMn_2O_6$	$C_{34}H_{18}FeO_{20}Re_4$	$C_{40}H_{22}FeO_{22}Re_4Ti$	$C_{32.50}H_{29}Cl_3Fe_2O_8Re_2$
fw	650.25	1547.13	1703.13	1138.01
cryst syst	monoclinic	triclinic	triclinic	monoclinic
space group	*Pn*	$P\bar{1}$	$P\bar{1}$	*C*2/*c*
cryst color	dark red	red-brown	dark brown	red
cryst dimensions, mm	0.36 × 0.30 × 0.015	0.34 × 0.08 × 0.01	0.17 × 0.17 × 0.01	0.40 × 0.36 × 0.26
a, Å	11.9498(11)	15.5600(14)	10.7406(7)	22.2670(16)
b, Å	9.7620(9)	16.0269(14)	12.1924(8)	15.2017(11)
c, Å	12.9245(12)	16.5632(14)	18.4356(12)	21.6438(15)
α, deg	90	98.175(1)	90.9060(10)	90
β, deg	115.7030(10)	91.337(1)	94.7320(10)	100.1860(10)
γ, deg	90	90.100(1)	95.6650(10)	90
V, Å^3	1358.5(2)	4087.4(6)	2393.5(3)	7210.9(9)
Z	2	4	2	8
D_{calc}, g cm^{-3}	1.590	2.514	2.363	2.097
μ, mm^{-1}	1.485	12.227	10.607	7.751
T_{min}/T_{max}	0.978−0.590	0.885−0.348	0.727−0.215	0.133−0.069
θ range, deg	2.72 to 26.44	2.34 to 26.52	2.41 to 26.33	2.38 to 26.25
reflns collected	6873	22399	12826	18498
ind reflns/R(int)	3294/0.0264	14796/0.0532	8569/0.0308	6671/0.0367
R1/wR2 (all data)	0.0384/0.0829	0.0995/0.1568	0.0778/0.1520	0.0386/0.0927
R1/wR2 ($I > 2\sigma(I)$)	0.0317/0.0779	0.0545/0.1265	0.0503/0.1319	0.0346/0.0885
params/GOF	371/1.066	1064/0.997	608/1.025	431/1.156

sp^2-hybridized carbene carbon atom which defines a carbene plane (Re−C−(O(X))−C(Fc)). A second plane is that of the ferrocenyl Cp ring bonded to the carbene carbon, and ideally, because of *π*-conjugation, this should be coplanar with the carbene plane. This plane is rotated approximately 16° with respect to the carbene plane for **3b** (torsion angles Re(1)−C(10)−C(21)−C(25) and Re(4)−C(20)−C(28)−C(30) are −164.0(12) and 163.3(11)°, respectively) due to steric effects (Table 3). The longer Re···Re distance observed in **6**, however, allows the two carbene ligands to lie on the same side of the Re_2Cl_2 plane, with the ethoxy group of one carbene ligand stacked over and approximately parallel with the nearest Fc-Cp ring of the other, and with the Fc-Cp rings coplanar with the defined carbene plane (Re(1)−C(4)−C(9)−C(13) = −179.23(5)°,

(36) (a) Rabier, A.; Lugan, N.; Mathieu, R. *J. Organomet. Chem.* **2001**, *617 - 618*, 681–695. (b) Casey, C. P.; Kraft, S.; Powell, D. R.; Kavana, M. *J. Organomet. Chem.* **2001**, *617 − 618*, 723–736.
(37) Mashima, K.; Jyodoi, K.; Ohyoshi, A.; Takaya, H. *J. Chem. Soc., Chem. Commun.* **1986**, 1145–1146.
(38) Fischer, E. O.; Rustemeyer, P. *J. Organomet. Chem.* **1982**, *225*, 265–277. (b) Schubert, U.; Ackermann, K.; Rustemeyer, P. *J. Organomet. Chem.* **1982**, *231*, 323–334.

Re(2)−C(8)−C(19)−C(23) = −179.5(5)). The sterically hindered metallacycle formed by the bridging biscarbene ligand of **4b** results in significant rotations of the ferrocenyl planes with respect to the corresponding carbene plane, and the corresponding torsion angles, Re(2)−C(10)−C(21)−C(25) and Re(4)−C(20)−C(26)−C(30), are −21.6(19) and −48.6(17)°, respectively. The two complexes **3b** and **6** both have ethoxy substituents adopting an orientation with their methylene carbon atoms toward the metal carbonyl ligands, which is electronically favored.[39]

Complex **4b** has both the longest and the shortest Re−C(carbene) bond lengths. The axial substitution of the one carbene places the ligand *trans* to the $Re(CO)_5$ fragment, where negligible competition for π-back-donation from the Re atom is expected. A shorter bond length (2.059(13) Å) and higher bond order than the mean value reported for terminal alkoxycarbene ligands (2.098 Å)[40] is observed. In contrast, a significantly longer equatorial Re−C(carbene) bond distance of 2.178(11) Å corroborates the finding that the acyl resonance structure contributes predominantly to the carbene complex's structure (Figure 3). Even stronger support of this supposition is the fact that for both the equatorial and axial carbene ligands, the C(carbene)−O bond length is found to be 0.035−0.08 Å shorter than those of the corresponding ethoxycarbene complexes, irrespective of substitution site, as well as the near linear C(carbene)−O−Ti angles (161.3(8), 176.2(8)°). For the O−C(carbene)−C(ring) bond angle, **4b** shows significantly larger angles for both the equatorial and the axial carbene ligands (113.0(10)° and 112.8(11)°) compared to the smaller angles for **3b** and **6** (104.8(13)° and 104.9(12)°; 107.4(5)° and 107.6(5)°, respectively). This observation seems to indicate that the loss in electronic stability of the equatorial position is compensated for by the sterically more favorable axial coordination.

Conclusions

In this paper, we have described the synthesis of the first examples of multimetallic group VII transition metal (Mn, Re) carbene complexes, where all of the metals are in electronic contact with each other *via* the carbene carbon atom. The novel biscarbene complexes bridging the dirhenium nonacarbonyl moieties displayed unusual coordination sites, with a loss of the electronically favored equatorial positions resulting in sterically less demanding axial coordination. In contrast to the group VI transition metal analogues, the complex reaction mixture of the group VII metals resulted in the isolation and characterization of several secondary products: although the stabilization of hydroxycarbene or hydrido-acyl complexes of rhenium carbonyls is not easily achieved, the existence of these species was confirmed in **8** and in the composition of isolated secondary complexes.

Experimental Section

All manipulations involving organometallic compounds made use of Schlenk techniques, and operations were carried out under an inert atmosphere. Hexane, THF, and DCM were dried and deoxygenated by distillation prior to use. $[MnCp(CO)_3]$, $[Re_2(CO)_{10}]$, ferrocene, *n*-BuLi (1.6 mol/dm^3 solution in hexane), and titanocene dichloride were used as purchased. Triethyloxonium tetrafluoroborate was prepared according to literature procedures,[41] and TMEDA was distilled before use. Iodoferrocene was prepared according to Fish and Rosenblum's method.[12] Column chromatography using silica gel 60 (0.0063−0.200 mm) or neutral aluminum oxide 90 as the stationary phase was used for all separations. The columns were cooled by circulating ice-water through the column jackets. Melting points were not recorded due to decomposition during heating. NMR spectra were recorded on a Bruker AVANCE 500 spectrometer. ^{1}H NMR spectra were recorded at 500.139 MHz and ^{13}C NMR spectra at 125.75 MHz. The signal of the deuterated solvent was used as a reference, e.g., ^{1}H $CDCl_3$ 7.24 ppm and benzene-d_6 7.15 ppm and ^{13}C $CDCl_3$ 77.00 ppm and benzene-d_6 128.00 ppm. The product compounds were characterized using ^{1}H and ^{13}C NMR and IR spectroscopy as well as mass spectrometry. The NMR spectra of all of the manganese carbene complexes were recorded in deuterated benzene as a solvent, while $CDCl_3$ was employed for the rhenium complexes, with the exception of **7**. A spectrum of high quality could only be obtained in C_6D_6. Broadening of the signals of the manganese complexes **1** and **2** was observed. In the case of the rhenium complexes, slow decomposition of the products over time was observed. IR spectra were recorded on a Perkin-Elmer Spectrum RXI FT-IR spectrophotometer in dichloromethane as the solvent. Only the vibration bands in the carbonyl-stretching region (*ca.* 1600−2200 cm^{-1}) were recorded. Due to the low solubility of the complexes in the nonpolar solvent hexane, the IR spectra of all complexes were recorded in dichloromethane. For **3a** (a mixture of equatorial and axial $M_2(CO)_9$ systems), **3b** (*eq*-$M_2(CO)_9$), **4b** (a combination of an *eq*-$M_2(CO)_9$ and an *ax*-$M_2(CO)_9$ system), **5** (a combination of an *eq*-$M_2(CO)_9$ and an $M(CO)_5$ system), and **9** (*eq*-$M_2(CO)_9$), band overlap prevented band assignment. FAB-MS methods in a 3-nitrobenzyl alcohol matrix were employed to record the mass spectra of the complexes and were recorded on a VG 70SEQ Mass Spectrometer, with the resolution for FAB = 1000 in a field of 8 kV. Nitrobenzyl alcohol was used as a solvent and internal standard. No molecular ion peak (M^+) nor any other *m*/*z* peak could be identified for **1a**. Stepwise fragmentation of the carbonyl ligands followed by a loss of the terminal $M(CO)_n$ fragments was observed consistently for all of the complexes.

General Method for the Synthesis of Fischer Carbene Complexes 1, 2, 3b, 4−9. A mixture of 1.5 mol equiv *n*-BuLi (15 mmol, 10 mL) and 1.5 mol eq TMEDA (15 mmol, 2.27 mL) was added to a solution of ferrocene (1.86 g, 10.0 mmol) in hexane at RT under an inert N_2 atmosphere. The reaction mixture was heated under reflux for two hours, after which the hexane was removed under reduced pressure. The reaction mixture was cooled to −78 °C and redissolved in a minimum of THF, after which the metal carbonyl complex precursor was added (10 mmol). After continuous stirring for 2 h at low temperature, the reaction mixture was allowed to warm to room temperature, after which the solvent THF was evaporated. Dichloromethane was added at −30 °C, and a slight excess (10−15 mmol) of the oxonium salt Et_3OBF_4 or titanocene dichloride was added. After complete alkylation or metalation, monitored by thin layer chromatography, the solution was filtered through a short silica gel filter to remove the lithium salts, followed by column chromatography with gradient elution with hexane and dichloromethane. Crystallization was achieved by solvent layering of hexane on a dichloromethane solution of the product.

Preparation of 3a. FcI (5 mmol, 1.56) was stirred while adding *n*-BuLi (5.5 mmol, 1.5 M, 3.66 mL) in 40 mL of THF at −20 °C under an inert N_2 atmosphere. Stirring was continued for 2 h.

(39) Fernández, I.; Cossío, F. P.; Arrieta, A.; Lecea, B.; Mancheño, M. J.; Sierra, M. A. *Organometallics* **2004**, *23*, 1065–1071.

(40) Orpen, A. G.; Brammer, L.; Allen, F. H.; Kennard, O.; Watson, D. G.; Taylor, R. *J. Chem. Soc., Dalton Trans.* **1989**, S1.

(41) Meerwein, H. *Org. Synth.* **1966**, *46*, 113–115.

$[Re_2(CO)_{10}]$ (5 mmol, 3.26 g) was then added to the reaction mixture at −78 °C, resulting in a change of the reaction mixture to a darker color while stirring for 1 h. Stirring was then continued for an additional 30 min at RT. THF solvent was evaporated under reduced pressure. Et_3OBF_4 (6 mmol, 1.15 g) in dichloromethane was added to the reaction mixture at −30 °C and stirred until reaction completion. $LiBF_4$ salts were removed by filtering, and the reaction products were separated via column chromatography using hexane/dichloromethane (4:1) as an eluent. Recrystallization of the products was done by solvent layering (1:1) of hexane on a dichloromethane solution of the product.

[MnCp(CO)$_2${C(OEt)Fc}] (1a). Yield: 1.57 g (38%). Anal. Calcd for $MnFeC_{20}O_3H_{19}$: C, 57.5; H, 4.6. Found: C, 57.6; H, 4.3. ^{1}H NMR (C_6D_6): δ 4.16 (s, Mn-Cp, 5H), 4.83 (br, H3,3′, 2H), 4.58 (br, H4,4′, 2H), 4.12 (s, Fe-Cp, 5H), 4.80 (br, CH_2, 2H), 1.24 (br, CH_3, 3H). ^{13}C NMR (C_6D_6): δ 328.5 (C1), 232.0, 230.4 (Mn-CO), 95.9 (C2), 83.8 (Mn-Cp), 73.6 (C3,3′), 72.3 (C4,4′), 71.3 (Fe-Cp), 73.7 (CH_2), 14.8 (CH_3). IR (ν_{CO}, cm^{-1}): 1938 vs, 1862 s. FAB-MS ([M]$^+$ (g/mol), % relative abundance): n.o.

[π-Fe{C$_5$H$_4$C(OEt)MnCp(CO)$_2$}$_2$] (1b). Yield: 12.96 g (46%). Anal. Calcd for $Mn_2FeC_{30}O_6H_{28}$: C, 55.4; H, 4.3. Found: C, 56.0; H, 4.2. ^{1}H NMR (C_6D_6): δ 4.12 (s, Mn-Cp, 10H), 4.92 (dd, J = 1.8, 1.8 Hz, H3,3′, 4H), 4.57 (dd, J = 2.0, 1.8 Hz, H4,4′, 4H), 4.82 (q, J = 7.0 Hz, CH_2, 4H), 1.29 (t, J = 7.0 Hz, CH_3, 6H). ^{13}C NMR (C_6D_6): δ 336.5 (C1), 231.9 (Mn-CO), 96.5 (C2), 84.0 (Mn-Cp), 73.9 (C3,3′), 72.3 (C4,4′), 74.7 (CH_2), 15.3 (CH_3). IR (ν_{CO}, cm^{-1}): 1927 vs, 1858 s. FAB-MS ([M]$^+$ (g/mol), % relative abundance): 650, 35.

[MnCp(CO)$_2${C(OTiCp$_2$Cl)Fc}] (2a). Yield: 1.48 g (25%). Anal. Calcd for $MnFeTiC_{28}O_3H_{24}Cl$: C, 55.8; H, 4.0. Found: C, 56.3; H, 4.0. ^{1}H NMR (C_6D_6): δ 6.20 (s, Ti-Cp$_2$, 10H), 4.03 (s, Mn-Cp, 5H), 4.22 (br, H3,3′, 2H), 3.87 (br, H4,4′, 2H), 4.19 (s, Fe-Cp, 5H). ^{13}C NMR (C_6D_6): δ 321.8 (C1), n.o. (Mn-CO), 118.2 (Ti-Cp$_2$), n.o. (C2), 82.7 (Mn-Cp), 71.3 (C3,3′), 70.1 (C4,4′), 64.2 (Fe-Cp). FAB-MS ([M]$^+$ (g/mol), % relative abundance): 603, 15.

[{π-TiCp$_2$O$_2$-O,O′}{π-Fe(C$_5$H$_4$)$_2$-C,C′}[CMnCp(CO)$_2$}$_2$] (2b). Yield: 4.06 g (53%). Anal. Calcd for $Mn_2FeTiC_{36}O_6H_{28}$: C, 56.1; H, 3.7. Found: C, 56.8; H, 3.6. ^{1}H NMR (C_6D_6): δ 6.37 (s, Ti-Cp$_2$, 10H), 4.38 (s, Mn-Cp, 10H), 4.28 (dd, J = 1.7, 1.7 Hz, H3,3′, 4H), 3.99 (dd, J = 1.7, 1.7 Hz, H4,4′, 4H). ^{13}C NMR (C_6D_6): δ 338.4 (C1), 233.7 (Mn-CO), 117.7 (Ti-Cp$_2$), n.o. (C2), 85.7 (Mn-Cp), 69.3 (C3,3′), 68.2 (C4,4′). IR (ν_{CO}, cm^{-1}): 1922 vs, 1849 s. FAB-MS ([M]$^+$ (g/mol), % relative abundance): 770, 11.

[Re$_2$(CO)$_9${C(OEt)Fc}] (3a). Yield: 2.08 g (48%). Anal. Calcd for $Re_2FeC_{22}O_{10}H_{14}$: C, 30.5; H, 1.6. Found: C, 30.9; H, 1.6. ^{1}H NMR ($CDCl_3$): δ 4.92 (dd, J = 2.2, 1.8 Hz, H3,3′(*eq*), 2H), 4.91 (dd, J = 2.2, 2.0 Hz, H3,3′(*ax*), 2H), 4.75 (dd, J = 2.2, 2.2 Hz, H4,4′(*eq*), 2H), 4.66 (dd, J = 1.9, 1.9 Hz, H4,4′(*ax*), 2H) 4.24 (s, Fe-Cp(*eq*), 5H), 4.27 (s, Fe-Cp(*ax*), 5H), 4.67 (q, J = 6.7 Hz, CH_2(*eq*), 2H), 4.55 (q, J = 7.2 Hz, CH_2(*ax*), 2H),1.64 (t, J = 6.9 Hz, CH_3(*eq*,*ax* overlap), 6H). ^{13}C NMR ($CDCl_3$): δ 306.3 (C1(*eq*)), 275.6 (C1(*ax*)), 199.2, 199.1, 194.9, 193.1, 189.7 (Re-CO), 98.8 (C2(*eq*)), 96.1 (C2(*ax*)), n.o. (C3,3′), 73.2 (C4,4′(*eq*)), 72.6 (C4,4′(*ax*)), 70.7 (Fe-Cp(*eq*)), 70.4 (Fe-Cp(*ax*)), 76.3 (CH_2(*eq*)), 74.0 (CH_2(*ax*)), 14.8 (CH_3). IR (ν_{CO}, cm^{-1}): 2101 w, 2039 m, 1996 vs, 1970 m, 1938 m. FAB-MS ([M]$^+$ (g/mol), % relative abundance): 867, 17.

***eq,eq*-[π-Fe{C$_5$H$_4$C(OEt)Re$_2$(CO)$_9$}$_2$] (3b).** Yield: 5.07 g (33%). Anal. Calcd for $Re_4FeC_{34}O_{20}H_{18}$: C, 26.4; H, 1.2. Found: C, 26.3; H, 1.4. ^{1}H NMR ($CDCl_3$): δ 4.88 (dd, J = 3.9, 2.0 Hz, H3,3′, 4H), 4.63 (dd, J = 3.9, 2.0 Hz, H4,4′, 4H), 4.50 (q, J = 7.1 Hz, CH_2, 4H), 1.69 (t, J = 6.9 Hz, CH_3, 6H). ^{13}C NMR ($CDCl_3$): δ 307.7 (C1), 198.8, 194.6, 192.3, 189.2 (Re-CO), 102.0 (C2), 74.7 (C3,3′), 72.8 (C4,4′), 77.8 (CH_2), 14.8 (CH_3). IR (ν_{CO}, cm^{-1}): 2102 m, 2038 m, 1995 vs, 1968 sh, 1940 m. FAB-MS ([M]$^+$ (g/mol), % relative abundance): 1547, 11.

***ax*-[Re$_2$(CO)$_9${C(OTiCp$_2$Cl)Fc}] (4a).** Yield: 2.24 g (21%). Anal. Calcd for $Re_2FeTiC_{30}O_{10}H_{19}Cl$: C, 34.3; H, 1.8. Found: C, 34.7; H, 1.8. ^{1}H NMR ($CDCl_3$): δ 6.57 (s, Ti-Cp$_2$, 10H), 4.98 (br, H3,3′, 2H), 4.71 (br, H4,4′, 2H), 4.39 (s, Fe-Cp, 5H). ^{13}C NMR ($CDCl_3$): δ n.o. (C1), 178.9, 176.9 (Re-CO), 120.1, 118.9 (Ti-Cp$_2$), 85.1 (C2), 76.3 (C3,3′), 71.5 (C4,4′), 70.5 (Fe-Cp). IR (ν_{CO}, cm^{-1}): 2156 w, 2064 w, 2046 vs, 1985 s, 1929 m. FAB-MS ([M]$^+$ (g/mol), % relative abundance): 1052, 17.

***ax,eq*-[{π-TiCp$_2$O$_2$-O,O′}{π-Fe(C$_5$H$_4$)$_2$-C,C′}{CRe$_2$(CO)$_9$}$_2$] (4b).** Yield: 4.47 g (27%). Anal. Calcd for $Re_4FeTiC_{40}O_{20}H_{18}$: C, 28.8; H, 1.1. Found: C, 29.2; H, 1.0. ^{1}H NMR ($CDCl_3$): δ 6.71 (s, Ti-Cp$_2$, 10H), 4.97 (br, H3,3′, 4H), 4.76 (br, H4,4′, 4H). ^{13}C NMR ($CDCl_3$): δ 272.6 (C1), 199.8, 193.8, 192.5, 186.9, 186.3, 186.2 (Re-CO), 125.8 (Ti-Cp$_2$), 95.5 (C2), 74.1 (C3,3′), 72.2 (C4,4′). IR (ν_{CO}, cm^{-1}): 2098 m, 2084 w, 2046 vw, 2027 m, 2005 s, 1991 vs, 1958 m, 1933 m, 1919 m. FAB-MS ([M]$^+$ (g/mol), % relative abundance): n.o.

[Re$_3$(CO)$_{14}$H] (5). Yield: 0.76 g (8%). ^{1}H NMR ($CDCl_3$): δ −15.41 (s, Re−H, 1H). ^{13}C NMR ($CDCl_3$): δ 196.1, 190.6, 186.5, 186.3, 183.6, 178.9, 176.8 (Re-CO). IR (ν_{CO}, cm^{-1}): 2147 w, 2101 s, 2046 vs, 2016 m, 1989 vs, 1922 m. FAB-MS ([M]$^+$ (g/mol), % relative abundance): 952, 48.

***fac*-[(π-Cl)$_2$-(Re(CO)$_3${C(OEt)Fc}$_2$] (6).** Yield: 2.21 g (20%). Anal. Calcd for $Re_2Fe_2C_{30}O_8H_{28}Cl_2$: C, 32.9; H, 2.6. Found: C, 33.2; H, 2.8. ^{1}H NMR ($CDCl_3$): δ 4.78 (br, H3,3′, 4H), 4.68 (br, H4,4′, 4H), 4.39 (s, Fe-Cp, 10H), 4.29 (br, CH_2, 4H), 1.53 (br, CH_3, 6H). ^{13}C NMR ($CDCl_3$): δ n.o. (C1), 199.2, 191.9 (Re-CO), n.o. (C2), 74.0 (C3,3′), 71.8 (C4,4′), 70.7 (Fe-Cp), 76.3 (CH_2), 14.8 (CH_3). IR (ν_{CO}, cm^{-1}): 2101 m, 2036 m, 1991 s, 1936 m. FAB-MS ([M]$^+$ (g/mol), % relative abundance): 541, 48.

[Re(CO)$_5${C(O)Fc}] (7). Yield: 0.30 g (6%). Anal. Calcd for $ReFeC_{16}O_6H_9$: C, 35.6; H, 1.7. Found: C, 36.2; H, 1.6. ^{1}H NMR (C_6D_6): δ 4.49 (dd, J = 2.7, 2.4 Hz, H3,3′, 2H), 4.04 (dd, J = 2.8, 2.7 Hz, H4,4′, 2H), 3.85 (s, Fe-Cp, 5H). ^{13}C NMR (C_6D_6): δ 234.8 (C1), 191.9, 183.9, 181.6 (Re-CO), n.o. (C2), 80.4 (C3,3′), 72.7 (C4,4′), 69.7 (Fe-Cp). IR (ν_{CO}, cm^{-1}): 2140 m, 2038 m, 2010 s, 1975 vs, 1565 m (C═O). FAB-MS ([M]$^+$ (g/mol), % relative abundance): n.o.

[(π-H)$_2$-(Re(CO)$_4${C(O)Fc}$_2$] (8). Yield: 0.46 g (5%). ^{1}H NMR ($CDCl_3$): δ 9.93 (s, C(OH), 1H), 5.03 (br, H3,3′, 4H), 4.98 (br, H4,4′, 4H), 4.70 (br, Fe-Cp, 10H), −15.59 (s, Re−H, 1H). ^{13}C NMR ($CDCl_3$): δ 346.2, 231.5 (C1), 185.9 (Re-CO), n. o. (C2), 76.0 (C3,3′), 74.0 (C4,4′), 70.8 (Fe-Cp). IR (ν_{CO}, cm^{-1}): 2083 w, 2069 w, 2012 vs, 1985 sh, 1971 m, 1955 m, 1926 w, 1610 (C═O). FAB-MS ([M]$^+$ (g/mol), % relative abundance): 1022, 18.

***eq*-[Re$_2$(CO)$_9${C(OTiCp$_2$Cl)(Fc′CHO)}] (9).** Yield: 0.41 g (4%). ^{1}H NMR ($CDCl_3$): δ 9.97 (s, CHO, 1H), 6.56 (s, Ti-Cp$_2$, 10H), 4.91 (br, H3,3′(Fe-Cp-carbene), 2H), 4.78 (br, H3,3′-(Fe-Cp-CHO), 2H), 4.71 (br, H4,4′(Fe-Cp-carbene), 2H), 4.60 (br, H4,4′(Fe-Cp-CHO), 2H). ^{13}C NMR ($CDCl_3$): δ 287.0 (C1), 200.9, 195.7 (Re-CO), 178.9 (CHO), 120.2, 119.2 (Ti-Cp$_2$), n.o. (C2), 74.5 (C3,3′(Fe-Cp-carbene)), 73.2 (C3,3′(Fe-Cp-CHO)), 71.3 (C4,4′(Fe-Cp-carbene)), 69.6 (C4,4′(Fe-Cp-CHO)). IR (ν_{CO}, cm^{-1}): 2099 w, 2046 m, 2023 m, 1988 vs, 1953 m, 1917 s, 1883 w, 1684 (CHO). FAB-MS ([M]$^+$ (g/mol), % relative abundance): 1079, 15.

X-Ray Crystallography. The crystal data collection and refinement details for complexes **1b**, **3b**, **4b**, and **6** are summarized in Table 4. X-ray crystal structure analyses were performed using data collected at 20 °C on a Siemens P4 diffractometer with a Bruker SMART 1K CCD detector and SMART control software using graphite-monochromated Mo Kα radiation by means of a combination of φ and ω scans. Data were corrected for Lorenz polarization effects. Data reduction was performed using SAINT+,[42] and the intensities were corrected for absorption using SADABS.[43] The structures were solved by direct

(42) *SMART*, version 5.054; *SAINT*, version 6.45; *SADABS*, version 2.10; *SHELXTS*/*SHELXTL*, version 6.12; Bruker AXS Inc.: Madison, WI, 2001.

methods using SHELXTS[43] and refined by full-matrix least-squares using SHELXTL[43] and SHELXL-97.[43] In the structure refinements, all hydrogen atoms were added in calculated positions and treated as riding on the atom to which they are attached. All non-hydrogen atoms (except those in very low occupancy sites in **1b**) were refined with anisotropic displacement parameters. All isotropic displacement parameters for hydrogen atoms were calculated as $X \times U_{eq}$ of the atom to which they are attached; $X = 1.5$ for the methyl hydrogens and 1.2 for all other hydrogens. In structure **1b**, some disorder was observed with a minor (8(2)%) orientation of the molecule with the ethoxy and ferrocenyl group positions swapped. Where atoms for the two orientations approximately coincided, these were treated as single enities and assigned as for the major orientation. The additional iron and carbon atom positions needed to complete the minor ferrocenyl group were refined with isotropic displacement parameters. A site occupation factor for these atoms plus a second factor for the corresponding (nonoverlapped) atoms of the major orientation were refined but constrained to sum to 1.0.

(43) *SHELXS-97*; *SHELXL-97*; GM University of Göttingen: Göttingen, Germany, 1997.

Acknowledgment. This paper is dedicated to the memory of Prof. John R. Moss, 1943−2010.

Supporting Information Available: Crystallographic data for **1b**, **3b**, **4b**, and **6** in CIF format have been deposited and are available free of charge via the Internet at http://pubs.acs.org.